

Validation of a multiscale magneto-mechanical hysteresis model using multiaxial experiments

Mahmoud Rekik, Olivier Hubert, Laurent Daniel

► To cite this version:

Mahmoud Rekik, Olivier Hubert, Laurent Daniel. Validation of a multiscale magneto-mechanical hysteresis model using multiaxial experiments. 6th Biennial IEEE Conference on Electromagnetic Field Computation (CEFC 2014), May 2014, Annecy, France. 6th Biennial IEEE Conference on Electromagnetic Field Computation (CEFC 2014), 2014. <hal-01552444>

HAL Id: hal-01552444

<https://hal-centralesupelec.archives-ouvertes.fr/hal-01552444>

Submitted on 2 Jul 2017

HAL is a multi-disciplinary open access archive for the deposit and dissemination of scientific research documents, whether they are published or not. The documents may come from teaching and research institutions in France or abroad, or from public or private research centers.

L'archive ouverte pluridisciplinaire **HAL**, est destinée au dépôt et à la diffusion de documents scientifiques de niveau recherche, publiés ou non, émanant des établissements d'enseignement et de recherche français ou étrangers, des laboratoires publics ou privés.

Validation of a multiscale magneto-mechanical hysteresis model using multiaxial experiments

Mahmoud Rezik^{*†}, Olivier Hubert^{*§}, Laurent Daniel^{†‡}

^{*}LMT-Cachan (ENS Cachan/CNRS(UMR8535)/PRES Universud Paris) 61, avenue du Président Wilson, 94235 Cachan, France

[†]LGEP (CNRS(UMR8507)/SUPELEC/UPMC/Univ Paris-Sud) 11, rue Joliot-Curie, Plateau de Moulon, 91192 Gif-sur-Yvette, France

[‡]School of Materials, University of Manchester, M1 7HS, Manchester, UK

[§]corresponding author - hubert@lmt.ens-cachan.fr

Abstract—Magneto-mechanical coupling effects play a significant role in the performance of high speed electrical machines. In order to provide engineers with accurate design tools, magneto-elastic effects must be included into constitutive laws for magnetic materials. A multiscale magneto-mechanical model including hysteretic effects has recently been proposed. We propose in this paper to validate its formulation by comparisons to magnetic measurements carried out under biaxial mechanical loadings.

Index Terms—Magneto-mechanical couplings, multiscale modeling, hysteresis effects.

I. INTRODUCTION - MAGNETO-MECHANICAL EFFECTS

The present research is motivated by the design of rotors of high speed electrical machines. The increased power density of these devices requires a higher rotation speed leading to higher levels of centrifugal forces and stress in the rotor. Coupled magneto-mechanical models are required in order to take into account changes in the magnetic behavior when a high intensity multiaxial stress state is applied. In addition they must take into account the anisotropy of electrical laminations and hysteresis effects. A multiscale magneto-elastic model including hysteresis effects has recently been proposed [1]. It has been compared to uniaxial magneto-mechanical measurements in a previous work leading to a first set of parameters. A validation of the approach is proposed herein using magnetic measurements carried out under biaxial mechanical loading. The results are compared to the prediction of the multiscale modeling in terms of susceptibility, coercive field and losses.

II. MULTISCALE MODELING OF HYSTERETIC EFFECTS

The model is derived from a micro-mechanical description of reversible magneto-elastic behavior [2], [3], [4] in which three scales are considered: magnetic domain (α), grain (g) and polycrystalline (representative volume element - *RVE*) scale. Since this model always refers to equilibrium, modeling results must be compared to anhysteretic (reversible) experimental measurements. It has been recently extended to hysteretic (irreversible) phenomena [1].

A. Reversible part of the model

A polycrystalline ferromagnetic media can be considered as an aggregate of single crystals assembled following the orientation data. The microscopic model is written using the volumetric fraction f_α of each domain family α as internal variable. The potential energy (1) is defined for each magnetic domain family α as the sum of the magneto-crystalline (2),

magnetostatic (3), elastic (4) and configuration (5) energies, detailed hereafter.

$$W^\alpha = W_K^\alpha + W_H^\alpha + W_\sigma^\alpha + W_C^\alpha \quad (1)$$

$$W_K^\alpha = K_1(\gamma_1^2\gamma_2^2 + \gamma_2^2\gamma_3^2 + \gamma_3^2\gamma_1^2) + K_2(\gamma_1^2\gamma_2^2\gamma_3^2) \quad (2)$$

$$W_H^\alpha = -\mu_0\vec{H}^\alpha \cdot \vec{M}^\alpha \quad (3)$$

$$W_\sigma^\alpha = \frac{1}{2}\boldsymbol{\sigma}^\alpha : \mathbb{C}^{\alpha-1} : \boldsymbol{\sigma}^\alpha \quad (4)$$

$$W_C^\alpha = -\boldsymbol{\Sigma} : \boldsymbol{\epsilon}_\mu^\alpha \quad (5)$$

where $\vec{M}^\alpha = M_s\vec{\gamma}^\alpha$ is the magnetization vector of the domain family α (M_s : saturation magnetization), $\vec{\gamma}^\alpha$ denotes the direction of magnetization (γ_i^α : direction cosines) in the crystal frame. K_1 and K_2 are the magnetocrystalline energy constants. \vec{H}^α is the magnetic field at the domain scale. $\boldsymbol{\sigma}^\alpha$ is the stress tensor at the domain scale. \mathbb{C}^α denotes the stiffness tensor of a domain family (or grain $\mathbb{C}^g = \mathbb{C}^\alpha$). $\boldsymbol{\epsilon}_\mu^\alpha$ denotes the magnetostriction strain tensor of a domain family α , where λ_{100} and λ_{111} are the magnetostriction constants:

$$\boldsymbol{\epsilon}_\mu^\alpha = \frac{3}{2} \begin{pmatrix} \lambda_{100}(\gamma_1^2 - \frac{1}{3}) & \lambda_{111}\gamma_1\gamma_2 & \lambda_{111}\gamma_1\gamma_3 \\ \lambda_{111}\gamma_1\gamma_2 & \lambda_{100}(\gamma_2^2 - \frac{1}{3}) & \lambda_{111}\gamma_2\gamma_3 \\ \lambda_{111}\gamma_1\gamma_3 & \lambda_{111}\gamma_2\gamma_3 & \lambda_{100}(\gamma_3^2 - \frac{1}{3}) \end{pmatrix} \quad (6)$$

Homogeneous field and deformation assumptions lead to a definition of magneto static and elastic energies involving magnetic and mechanical loadings at the grain scale:

$$W_H^\alpha = -\mu_0\vec{H}^g \cdot \vec{M}^\alpha \quad (7)$$

$$W_\sigma^\alpha = -\boldsymbol{\sigma}^g : \boldsymbol{\epsilon}_\mu^\alpha \quad (8)$$

The configuration term W_C^α [8], [1] aims at taking account for the possible non randomness of the initial domain configuration due for instance to plastic deformation or to significant demagnetizing surface effects. This configuration energy is chosen equivalent to the effect of a - fictitious - residual stress uniform within the material so that its introduction keeps the magnetization null at zero applied field. When an external stress is applied to the material, the modification of the initial domain structure can lead on the other hand to increasing

demagnetizing field \vec{H}_d^g that should be superposed to the applied field to define the effective field at the grain scale. The following definition for \vec{H}_d^g has recently been proposed [1], [9] :

$$\vec{H}_d^g = \eta(N^g - \frac{1}{3})\vec{M}^g \quad (9)$$

where η is a material parameter, \vec{M}^g is the magnetization at the grain scale, and N^g defines the stress-demagnetization effect given by equation 10. Its value belongs to the interval [0 1] and is 1/3 when no stress is applied:

$$N^g = \frac{1}{1 + 2 \exp(-K \sigma_{eq})} \quad (10)$$

K is a material parameter, σ_{eq} is the equivalent stress corresponding to a multiaxial stress σ . Its expression recalled in equation 11 can be found in [6]:

$$\sigma_{eq} = \frac{3}{2} \vec{h} \cdot (\sigma - \frac{1}{3} \text{trace}(\sigma) \mathbf{I}) \cdot \vec{h} \quad (11)$$

where \vec{h} denotes the direction of magnetization and \mathbf{I} the second order identity tensor.

At the grain scale, the volume fraction f_α of a family domain α is calculated thanks to a statistical approach (Boltzmann function - 12). The calculation does not require any minimization of the potential energy.

$$f_\alpha = \frac{\exp(-A_s \cdot W^\alpha)}{\int_\alpha \exp(-A_s \cdot W^\alpha) d\alpha} \quad (12)$$

with

$$A_s = \frac{3\chi_0}{\mu_0 M_s^2} \quad (13)$$

χ_0 , M_s and μ_0 are the initial susceptibility, the saturation magnetization and the vacuum permeability respectively.

Assuming that the elastic behavior is homogeneous within a grain, the magnetostriction strain of a single crystal is written as the mean magnetostriction strain over the domains (14). The magnetization in a grain is defined as well (15).

$$\epsilon_\mu^g = \int_\alpha f_\alpha \epsilon_\mu^\alpha d\alpha \quad (14)$$

$$\vec{M}^g = \int_\alpha f_\alpha \vec{M}^\alpha d\alpha \quad (15)$$

The possible directions $\vec{\gamma}^\alpha$ of domains α are described through the mesh of a unit radius sphere (N unit vectors \vec{x}_n). A 10242 points mesh has been used in the present study. The magnetic behavior at polycrystalline scale is defined as the average value of magnetization (16). A local demagnetizing field in each grain due to the magnetization of the surrounding grains can be introduced: the magnetic field at the grain scale \vec{H}^g is defined as a function of the external field, the mean secant equivalent susceptibility of the material χ_m , ($\chi_m = M/H$) and the difference between the mean magnetization \vec{M} and the magnetization at the grain scale \vec{M}^g (17). It

has to be complemented by the stress demagnetizing field if stress is considered. The elastic behavior is obtained thanks to a self-consistent homogenization scheme. The macroscopic magnetostriction strain (18) is estimated using the Eshelby's solution and considering the local magnetostriction as a free strain; \mathbb{B} denotes the fourth order stress concentration tensor.

$$\vec{M} = \langle \vec{M}^g \rangle \quad (16)$$

$$\vec{H}^g = \vec{H} + \frac{1}{3 + 2\chi_m} (\vec{M} - \vec{M}^g) + \vec{H}_g^d \quad (17)$$

$$\epsilon_\mu = \langle {}^t \mathbb{B} : \epsilon_\mu^g \rangle \quad (18)$$

The magnetostriction strain at grain scale is elastically incompatible and creates a stress that changes the magneto-elastic energy term (self-stress). The stress at the grain scale σ^g is derived from the implicit equation (19).

$$\sigma^g = \mathbb{B} : \sigma + \mathbb{C}^{acc} : (\epsilon_\mu - \epsilon_\mu^g) \quad (19)$$

with $\mathbb{C}^{acc} = (\mathbb{C}^g)^{-1} + (\mathbb{C}^0 : ((\mathbb{S}^{Esh})^{-1} - \mathbf{I}))^{-1}$. \mathbb{C}^g and \mathbb{C}^0 are the stiffness tensor of the grain and of the effective media respectively. Since a self-consistent scheme is usually chosen, \mathbb{C}^0 refers to the self-consistent stiffness tensor. σ is the macroscopic stress. \mathbb{S}^{Esh} is the so-called Eshelby tensor.

B. Irreversible part of the model

The dissipation can be introduced by adding an irreversible contribution to the magnetic field, as proposed by Hauser under no applied stress [5]. The dissipation is introduced at the single crystal scale by adding an irreversible contribution \vec{H}_{irr}^g to the anhysteretic magnetic field \vec{H}_g (17):

$$\|\vec{H}_{irr}^g\| = \delta \left(\frac{k_r}{\mu_0 M_s} + c_r \|\vec{H}^g\| \right) \left[1 - \kappa^g \exp\left(-\frac{k_a}{\kappa^g} \|\vec{M}^g - \vec{M}_{prev}^g\| \right) \right] \quad (20)$$

\vec{H}_{irr}^g is assumed to be parallel to \vec{H}_g . δ is equal to ± 1 , depending on whether the material is being loaded or unloaded (the sign of δ is changed each time there is an inversion in the loading direction). k_r , c_r , k_a and κ^g are material parameters. The value of κ^g changes each time there is an inversion in the loading direction. The new value of κ^g is calculated from the previous value κ_o^g according to equation 21. The initial value κ_i^g of κ^g is a material constant. \vec{M}_{prev}^g is the value of \vec{M}^g at the previous inversion of the loading direction.

$$\kappa^g = 2 - \kappa_o^g \exp\left(-\frac{k_a}{\kappa_o^g} \|\vec{M}^g - \vec{M}_{prev}^g\| \right) \quad (21)$$

In the case of a purely magnetic loading, an inversion of loading direction is detected at instant t when $\Delta H(t) \cdot \Delta H(t + dt) < 0$ ¹.

It must be underlined that parameter k_r of Hauser's relation (20) is defining the maximum coercive field H_c^{max} ($H_c^{max} = \frac{k_r}{\mu_0 M_s} = \|\vec{H}_{irr}^g\|_{\vec{M}^g \rightarrow \infty; \vec{H}^g = \vec{0}}$). In our modeling approach,

¹More generally an inversion of magneto-mechanical loading direction in a grain g can be defined at instant t using the average free energy $W^g = \int_\alpha W^\alpha d\alpha$ of grain g when $\Delta W^g(t) \cdot \Delta W^g(t + dt) < 0$

the coercive field is assumed to show the same dependence to the applied stress than the configuration demagnetizing field. Indeed the coercive field is linked to the configuration effect because the probability of encountering pinning centre depends on the space between domain walls. A domain family fraction grow increases the demagnetizing field and consequently reduces the space between domain wall. This decrease reduces the average swept area during their displacement, that reduces the probability of encountering pinning centre. The following expression has been proposed for k_r :

$$k_r = k_{r0} \left(1 - \zeta \left(N^g - \frac{1}{3}\right)\right) \quad (22)$$

k_{r0} and ζ being two other material constants.

III. VALIDATION USING 2D EXPERIMENTS

The material parameters can be identified from anhysteretic measurements at low field under uniaxial stress, from a magnetostriction measurement at high field for two perpendicular directions and from a major hysteresis loop under uniaxial stress too. Some comparisons between uniaxial experiments with a non-oriented 3%Si-Fe sheet and modeling are available in [1]. Parameters used are recalled in table I.

TABLE I
PARAMETERS OF THE MULTISCALE MODELING IDENTIFIED THANKS TO UNIAXIAL EXPERIMENTS.

| Param. | M_s | $K_1;K_2$ | $\lambda_{100};\lambda_{111}$ | $C_{11};C_{12};C_{44}$ | χ_0 | | | |
|--------|-------------------|--------------------|-------------------------------|------------------------|----------|-------|-------------------|----------------|
| Value | $1.61e^6$ | 38;0 | 23;-4.5 | 202;122; 229 | 2030 | | | |
| Unit | A/m | kJ.m^{-3} | ppm | GPa | - | | | |
| Param. | K | Σ_c | η | k_r^0 | ζ | c_r | k_a | κ_{ini} |
| Value | $4.14e^{-2}$ | 20 | $2e^{-4}$ | 150 | 2.9 | 0.1 | $15e^{-6}$ | 1 |
| Unit | MPa^{-1} | MPa | - | J.m^{-3} | - | - | m.A^{-1} | - |

A validation of the model is proposed in this paper using magnetic measurements carried out with the same material submitted to biaxial stress (extensive description of experimental set-up and experimental results are available in [7]). These non-conventional experiments are performed on cross-shaped iron-silicon thin sheets using a multiaxial testing machine. A local frame (1,2) is attached to the sheet with direction 1 and 2 corresponding to the rolling direction (RD) and to the transverse direction (TD) respectively and corresponding to the eigen-directions of stress tensor σ with principal values (σ_1, σ_2). Magnetic field is applied along RD and at 45° between RD and TD. These two configurations give an insight into some aspects of material anisotropy and allow testing the robustness of the model. Both anhysteretic and dissipative magnetic responses to magneto-mechanical loadings have been recorded (magnetic susceptibility χ , coercive field H_c , energy losses per cycle W). But the effect of biaxial stress on these behaviors will not be discussed here due to length limitation. Lecturers may refer to [9] for extensive discussion about these results. The polycrystalline aggregate considered in the modeling is an orientation data file made of 396 orientations extracted from EBSD (Electron back-scattered diffraction) measurements.

A. Influence of a biaxial stress on the anhysteretic behaviour

The influence of a biaxial stress on the anhysteretic behaviour is discussed first in terms of secant susceptibility $\chi = (M/H)$. Fig.1 and 2 plot the experimental vs. modeled secant susceptibility in the (σ_1, σ_2) plane for magnetic loading of magnitude $H=200$ A/m along RD and 45° respectively.

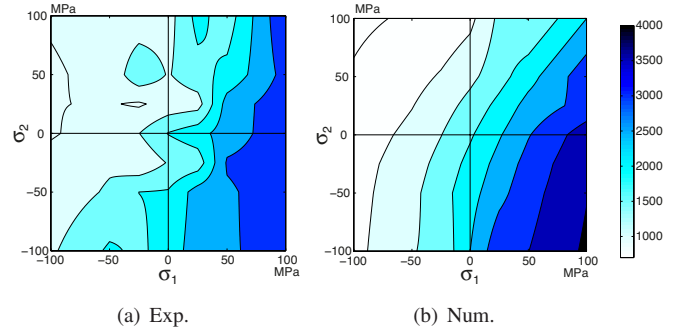


Fig. 1. Exp. vs Num. secant magnetic susceptibility χ in the stress plane for a magnetic loading along RD - $H=200\text{A/m}$.

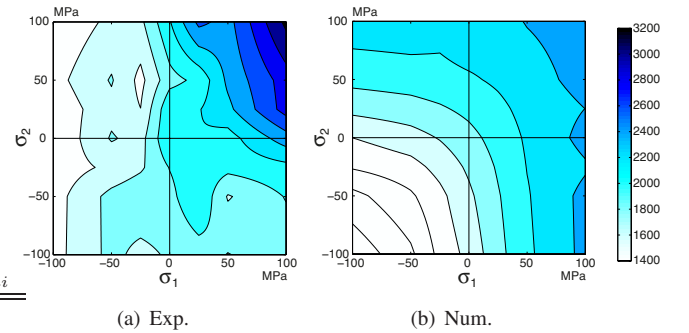


Fig. 2. Exp. vs Num. secant magnetic susceptibility χ in the stress plane for a magnetic loading along 45° - $H=200\text{A/m}$.

Experimental data and model are in good agreement for $\vec{H} // \text{RD}$, especially concerning the major effect of stress in the direction of applied field. Isovalues exhibit in both cases lines whose slope is about 2. When the field is oriented at 45° , the iso-values turn along lines given by $\sigma_1 + \sigma_2 = Cte$ in accordance with an insensitivity of magnetic properties to pure shear stress. The model leads to the same tendencies even if iso-values lines tend to form more hyperbola than straight lines. As for experiments, the values along the $\sigma_1 = \sigma_2$ axis of simulations correspond to each other. This result is in accordance with a low macroscopic in plane anisotropy of the sheet (associated to the FDO used for simulations). It will be confirmed by the measurement and modeling of other magnetic quantities.

B. Influence of a biaxial stress on the hysteretic behaviour

Fig.3 and 4 plot the experimental vs. modeled coercive field H_c in the (σ_1, σ_2) plane for a magnetic loading along RD and 45° respectively. It has been measured on magnetic cycles (experimental and modeled) of maximal magnitude $H_m=650$ A/m.

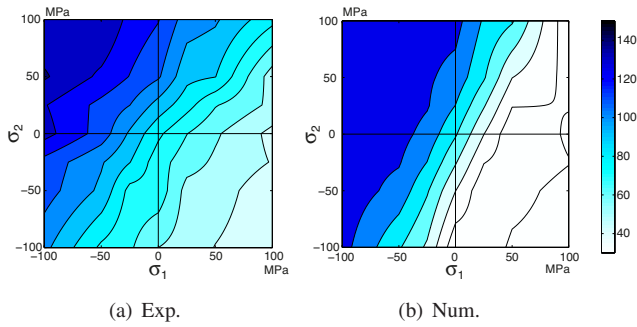


Fig. 3. Exp. vs. Num. coercive field strength (A/m) in the stress plane for a magnetic loading along RD - $f=5\text{Hz}$ for experiment.

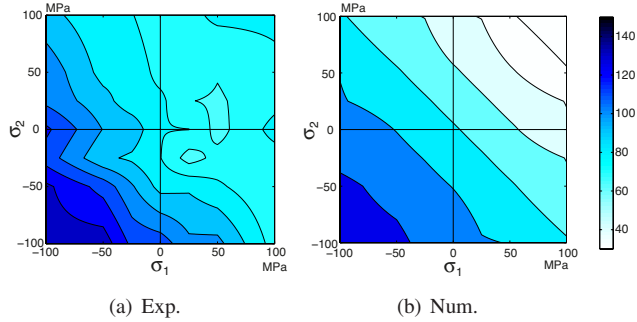


Fig. 4. Exp. vs. Num. coercive field strength (A/m) in the stress plane for a magnetic loading along 45° - $f=5\text{Hz}$ for experiment.

For magnetic field applied along RD , iso- H_c values form lines for measurements and modeling. The slope of these lines seems a few lower for experiments than for modeling. Variation levels are good accordance. Iso- H_c values for $\vec{H}/45^\circ$ form lines too in accordance with insensitivity for shear stress (as observed for susceptibility). Results obtained are satisfying even if variation levels are a few higher for modeling in the btraction area ($\sigma_1 > 0, \sigma_2 > 0$).

The energy losses per cycle W in the (σ_1, σ_2) plane are next addressed for the two magnetic field loading directions in Fig.5 and 6 respectively. Cycles areas have been measured on magnetic cycles (experimental and modeled) of the same maximal magnitude than for coercive field measurements ($H_m=650$ A/m). Despite the model predicts variations that are much higher than experimentally observed, experimental and model indicate both a higher level of energy loss along the $\sigma_1 = \sigma_2$ axis for \vec{H}/RD . Symmetry with respect to $\sigma_1 = \sigma_2$ axis is not observed in the experimental results obtained for $\vec{H}/45^\circ$. This is in contradiction with susceptibility and coercive field experimental results. Quality of measurement may be partly at the origin of discrepancies observed. The trend of multiscale model to overestimate the magnetization level at the knee of magnetization curve [1] is another source of discrepancy.

IV. CONCLUSION - PERSPECTIVES

Recent developments in the multiscale model include the consideration of non-monotonic effects of stress on the magnetic susceptibility and the description of the magnetic hystere-

sis. In addition to the conventional materials parameters from

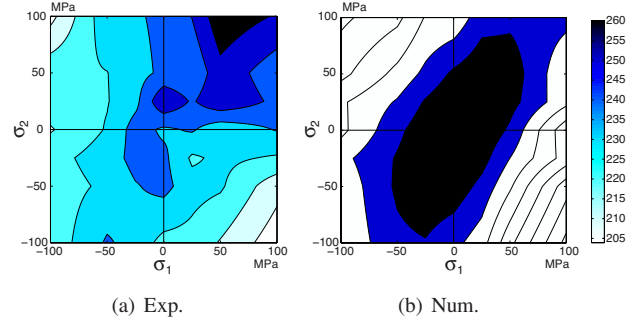


Fig. 5. Exp. vs. Num. energy losses per cycle ($\text{J}\cdot\text{m}^{-3}$) in the stress plane for a magnetic loading along RD - $f=5\text{Hz}$ for experiment.

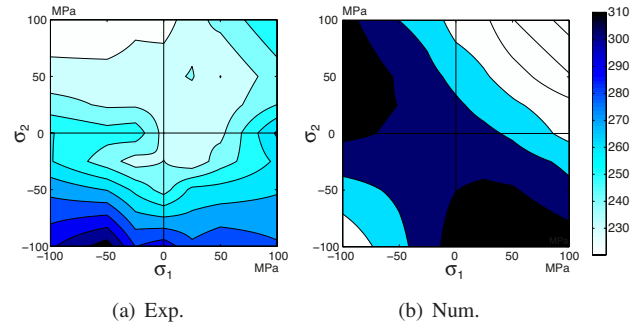


Fig. 6. Exp. vs. Num. energy losses per cycle ($\text{J}\cdot\text{m}^{-3}$) in the stress plane for a magnetic loading along 45° - $f=5\text{Hz}$ for experiment.

the literature, the model uses three parameters for modeling the anhysteretic behavior and six additional parameters for modeling hysteresis. It allows at present an accurate description of coercive field whatever the magneto-mechanical loading. The modeling of losses remains imperfect. Discrepancies seem partly due to uncertainties of experimental results.

REFERENCES

- [1] L. Daniel *et al.*, "A multiscale model for magneto-elastic behaviour including hysteresis effects", *Arch. Appl. Mech.*, DOI:10.1007/s00419-014-0863-9, 2014.
- [2] N. Buiron *et al.*, "Influence of the texture of soft magnetic materials on their magneto-elastic behaviour", *J. Phys. IV*, vol.11 pp. 373-377, 2001.
- [3] L. Daniel *et al.*, "Reversible magneto-elastic behavior: a multiscale approach", *J. Mech. Phys. Solids*, vol. 56 no.3, pp. 1018-1042, 2008.
- [4] N. Galopin and L. Daniel, "A constitutive law for magnetostrictive materials and its application to Terfenol-D single and polycrystals", *Eur. Phys. J. - Appl. Phys.*, vol.42 pp.153-159, 2009.
- [5] H. Hauser, "Energetic model of ferromagnetic hysteresis: Isotropic magnetization" *J. Appl. Phys.*, vol.96 no.5, pp. 2753-2767, 2004.
- [6] O. Hubert and L. Daniel, "Energetical and multiscale approaches for the definition of an equivalent stress for magneto-elastic couplings" *J. Magn. Magn. Mat.*, vol.323 no.13, pp. 1766-1781, 2011.
- [7] M. Rezik *et al.*, "Influence of a multiaxial stress on the reversible and irreversible magnetic behaviour of a 3%Si-Fe alloy", *Int. J. Appl. Electromagn. Mech.*, vol.44 (3-4) pp. 301-315, 2014.
- [8] O. Hubert and L. Daniel, "Multiscale modeling of the magneto-mechanical behavior of grain-oriented silicon steels", *J. Magn. Magn. Mat.*, vol.320, no7, pp. 1412-1422, 2008.
- [9] M. Rezik, L. Daniel, O. Hubert, "Equivalent stress model for magnetic hysteresis losses under biaxial loading", *IEEE Trans. Magn.*, vol.50 no.8, pp.1-4, 2014